Geophysical Research Letters

RESEARCH LETTER
10.1029/2020GL089824

Special Section:
Community Earth System Model version 2 (CESM2) Special Collection

The Role of the Mean State on MJO Simulation in CESM2 Ensemble Simulation

Daehyun Kang[1], Daehyun Kim[1], Min-Seop Ahn[2], Richard Neale[3], Jiwoo Lee[2], and Peter J. Gleckler[2]

[1]Department of Atmospheric Sciences, University of Washington, Seattle, WA, USA, [2]Lawrence Livermore National Laboratory, Livermore, CA, USA, [3]National Center for Atmospheric Research, Boulder, CO, USA

Abstract This study examines the role of the mean state in the propagation of the Madden-Julian oscillation (MJO) over the Maritime Continent (MC). We use an ensemble of simulations made with a single model—the Community Earth System Model version 2—to assess the effect of the mean state that is unaffected by that of model components such as parameterization schemes. Results show that the background meridional moisture gradient is much steeper over the MC region in the periods with a stronger MJO propagation. Column water vapor budget of the MJO strongly suggests that the simulated mean state affects MJO via its impacts on moisture dynamics—a greater advection of mean moisture by MJO wind in the MC region is responsible for the anomalous MJO activity.

Plain Language Summary The Madden-Julian oscillation (MJO) is a planetary-scale, eastward moving envelope of anomalous convection in the tropics. It is the dominant mode of sub-seasonal variability in the tropics. Unfortunately, an accurate representation of the MJO has historically been a challenging task for many, if not most, global climate models. The mean state distribution of atmospheric moisture has been highlighted as a key aspect affecting the simulation of MJO propagation in many recent modeling studies. When many different models are compared, however, it is difficult to isolate the role of the mean state because different models use different parameterizations of moist physics that affect both the mean state and the MJO directly. In this study, we examine the relationship between the mean state and MJO propagation in an ensemble of simulations made with a single coupled model—the Community Earth System Model version 2 (CESM2). Each ensemble member differs only in its initial conditions and thus the parameterizations and resolution are identical. We found that MJO propagation over the MC in CESM2 is strongly affected by the background meridional moisture gradient (MMG), with MJO propagation being enhanced in the periods with a steeper MMG.

Key Points:

- Each ensemble in the Community Earth System Model version 2 historical simulation shows a marked low-frequency variability in Madden-Julian oscillation (MJO) propagation across the Maritime Continent (MC)
- Simulation periods with enhanced MJO propagation across the MC exhibit a steeper background meridional moisture gradient (MMG) around the MC
- The steeper background MMG strengthens moisture recharging to the east of MJO, leading its eastward propagation

Supporting Information:

- Supporting Information S1

Correspondence to:
D. Kim,
daehyun@uw.edu

Citation:
Kang, D., Kim, D., Ahn, M. S., Neale, R., Lee, J., & Gleckler, P. J. (2020). The role of the mean state on MJO simulation in CESM2 ensemble simulation. *Geophysical Research Letters*, *47*, e2020GL089824. https://doi.org/10.1029/2020GL089824

Received 16 JUL 2020
Accepted 23 NOV 2020

1. Introduction

The Madden-Julian oscillation (MJO, Madden & Julian, 1971, 1972), the dominant mode of tropical intraseasonal variability, is an eastward propagating, planetary-scale envelop of anomalous convection coupled with circulation anomalies throughout the troposphere. The convection and circulation anomalies associated with the MJO exert substantial impacts on various weather and climate phenomena (Zhang, 2013), and thereby the MJO provides a major source of predictability in the sub-seasonal-to-seasonal time scales (Jones et al., 2004; Neena et al., 2014). Unfortunately, an accurate representation of the MJO has historically been a challenging task for many, if not most, global climate models (Ahn et al., 2017; Hung et al., 2013; Jiang et al., 2015; Kim et al., 2009).

Linear perturbation theory (Holton & Hakim, 2013) is a widely accepted framework to study the dynamics of wave-like fluid motions. The basic state around which the wave perturbations are defined is almost always a key aspect of the system determining the fluid wave motion characteristics such as phase speed and growth rate. Similarly, it has long been speculated that poor simulation of the MJO by general circulation models (GCMs) is due to the biases in the basic state (Ahn, Kim, Kang, et al., 2020; Gonzalez & Jiang, 2017; Inness et al., 2001; Jiang, 2017; Kim et al., 2009; Slingo et al., 1996). For example, Slingo et al. (1996) found that models with more realistic simulation of the climatological seasonal cycle tend to exhibit better intraseasonal variability.

There are at least two factors that make characterizing the role of the GCM basic state in the MJO particularly challenging. From a modeling point of view, the cumulus parameterization has substantial impacts on

simulated MJOs (see Kim & Maloney, 2017 for a review), and affects the mean state (Ahn et al., 2019; Kim et al., 2011; Mapes & Neale, 2011). Because changes in the convection scheme can affect the MJO both *directly* by altering how convection interacts with its large-scale environment and *indirectly* via their impacts on the basic state, separating the latter from the former is a non-trivial task (e.g., Peatman et al., 2018). In a similar vein, the atmosphere-ocean feedback, which is also known as a crucial factor for realistic MJO simulation, affects not only the MJO-related surface flux anomalies but also the meridional gradient of mean state moisture around the equator (DeMott et al., 2019).

From a theoretical point of view, it has remained elusive as to which aspects of the basic state are key to an accurate simulation of the MJO. Reflecting on the lack of consensus, previous studies have emphasized, rather empirically, the distribution of mean precipitation (Kim et al., 2009; Slingo et al., 1996) and the westerly basic state wind in the equatorial Indo-Pacific warm pool (Inness et al., 2001). Kim et al. (2011), who suggested that the conventional ways of improving the MJO tended to degrade the mean state, examined pattern correlations between the simulated and observed seasonal mean rain rate distributions. Ling et al. (2017) suggested that GCMs with poor MJO performance (as gauged by conventional metrics) had infrequent MJO events, which occurs only when the mean state is occasionally supportive of the MJO. However, they did not specify the aspects of the basic state that set favorable conditions for MJO emergence.

Recent advances in connecting the MJO and mean state have been guided by the moisture mode theory that explains the propagation and maintenance of the MJO by those of column-integrated moisture anomalies (Adames & Kim, 2016; Raymond & Fuchs, 2009; Sobel & Maloney, 2012, 2013). Many studies have suggested that the horizontal gradient of mean moisture around the Maritime Continent (MC) is the aspect of the mean state that is key to a skillful MJO simulation (Ahn, Kim, Kang, et al., 2020; Gonzalez & Jiang, 2017; Jiang, 2017). It was shown that models with a relatively good MJO simulation skill tend to have a more realistic background moisture distribution with a steeper horizontal moisture gradient in the vicinity of the MC region (Gonzalez & Jiang, 2017). With the steeper moisture gradient, the good MJO models better represent horizontal moisture advection (Jiang, 2017), the process responsible for MJO's eastward movement (Maloney, 2009; Kiranmayi & Maloney, 2011; Kim et al., 2014; Sobel et al., 2014). Ahn, Kim, Kang, et al. (2020) showed that the models participating in the CMIP6 tend to better simulate MJO propagation over the MC than the CMIP5 models and attributed the improvement to those in the horizontal gradient of background moisture near the MC area.

While the above-mentioned model intercomparison studies have shown a statistically robust relationship between the mean state moisture gradient and the MJO, it remains unclear how much of the inter-model difference in MJO simulation fidelity is due to the difference in the mean state. Because the models included in the intercomparison studies differ in their parameterization schemes (notably the cumulus scheme), it is difficult to isolate the effects of the mean state from those of the parameterization schemes. In this study, to assess the role of the background moisture gradient on MJO propagation that is independent of the effect of model physics and other model configurations, we use a 10-member ensemble simulation made with a single model that simulates a reasonable MJO. Specifically, this study addresses the following two questions: i) Do MJO characteristics vary substantially in time in long-term simulations made with a single model? If so, ii) can the low-frequency variability in MJO characteristics be explained by variations in the background moisture gradient? It will be shown that the eastward propagation of the MJO over the MC region is much more pronounced when the meridional gradient of mean moisture near the MC region is anomalously steeper.

This manuscript is organized as follows. Section 2 describes the data and methodology employed in our study. In Section 3, we examine MJO propagation during the historical period (1850–2014) based on the moisture mode framework, then the basic state affecting the low-frequency MJO variability is identified. Section 4 presents the summary and conclusions.

2. Data and Method

2.1. Data Set

The primary data set used in this study is the Coupled Model Intercomparison Project phase 6 (CMIP6; Eyring et al., 2016) historical simulations made with the Community Earth System Model version 2 (CESM2; Danabasoglu et al., 2020). The historical simulation covers the period from 1850 to 2014 and is driven by

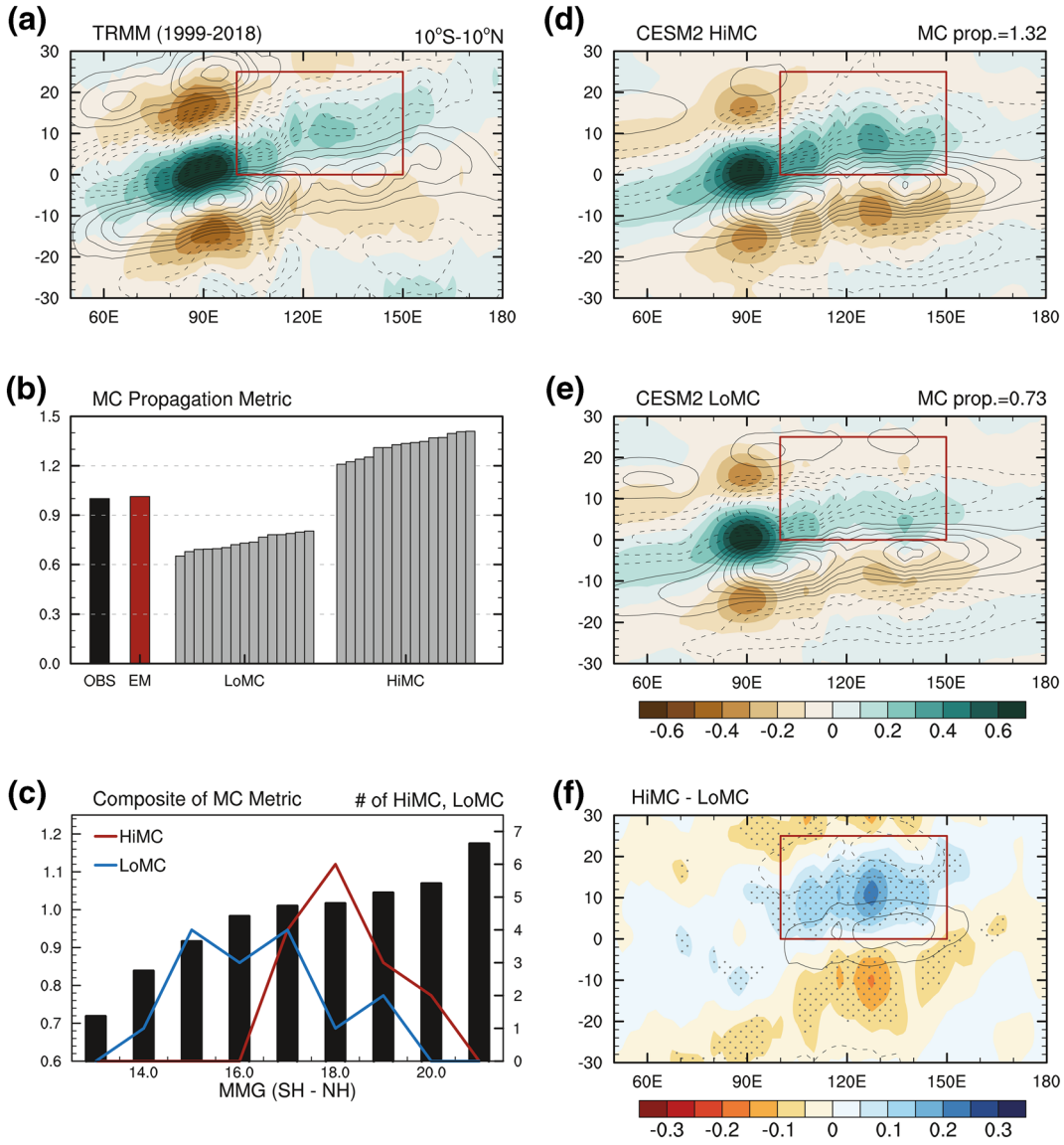

Figure 1. (a) Longitude-time evolution of 20–100 day band pass-filtered TRMM precipitation (shaded; the unit is mm day^{-1}) and ERA5 column-integrated moisture tendency (contour; kg m^{-2} s^{-1}) near the equator (10°S-10°N) regressed onto the precipitation averaged in the IO base point (85°E-95°E, 5°S-5°N) for 1999–2018. The red boxes indicate a domain for the MC propagation metric. (b) The MC propagation metric of TRMM, the ensemble mean of the CESM2 historical simulation for 1850–2014, and each 20-year moving windows in HiMC and LoMC in ascending order. (c) Composite of the MC metric binned by MMG index (unit: 10^6 kg m^{-3}, interval of the bin is 1) in the 1,450 windows (bars, left *y*-axis), and the number of HiMC and LoMC windows in each bin (lines, right *y*-axis). (d, e) Same as (a), but for composites of (d) the HiMC and (e) the LoMC of CESM2. (f) Difference between HiMC and LoMC. Areas with black dots in (f) indicate that a statistically significant difference between HiMC and LoMC (*p*-value = 0.01) using the two-sided Student's *t*-test adjusted by the FDR (α_{FDR} = 0.1).

best estimates of historical anthropogenic emissions. CESM2 realistically captures the observed characteristics of the eastward propagation of MJO (e.g., Ahn, Kim, Kang, et al., 2020, also see Figure 1). We use ten ensemble members (E1–E10) that are available in the CMIP6 archive, which differ from each other only in their initial conditions. The Tropical Rainfall Measuring Mission 3B42 version 7 (TRMM 3B42v7; Huffman et al., 2007) precipitation product is used for verifying MJO simulation fidelity for a recent 20-year period (1999–2018). Atmospheric field variables are obtained from the fifth generation of the European Centre for Medium-Range Weather Forecasts (ECMWF) reanalysis (ERA5; Hersbach et al., 2019). All analysis is performed after interpolating data onto a 2.5 longitude × 2.5 latitude horizontal grid and 6 vertical levels

from 1,000 to 100-hPa (1,000, 850, 700, 500, 250, and 100). We focus on boreal winter (November to April), during which the eastward propagation of the MJO is most pronounced.

3. Methods

To diagnose MJO propagation characteristics, intraseasonal (20–100 days) precipitation anomalies near the equator (10°S-10°N) are regressed onto intraseasonal precipitation anomalies averaged over the equatorial Indian Ocean (IO; 85°E-95°E, 5°S-5°N) and plotted in a lag-longitude diagram (e.g., Figure 1). We use the "MC propagation metric" of Ahn, Kim, Kang, et al. (2020) that is designed to quantitatively assess the robustness of the MJO's eastward propagation over the MC. The metric is obtained by averaging positive regression coefficients in the lag-longitude diagram over lag days 0–25 and longitudes 100°E-150°E (red box in Figure 1) and then normalizing the resulting value by the corresponding value from observations. Ahn, Kim, Kang, et al. (2020) demonstrated that the metric is useful in assessing GCM simulation fidelity of the MJO's propagation over the MC region.

The column-integrated moisture budget of the MJO is analyzed following Adames (2017), who normalized the budget terms by the convective moisture adjustment time scale ($\overline{\tau_c}$) in order that the moisture budget is more relevant to precipitation anomalies.

$$\frac{1}{\overline{\tau_c}}\frac{\partial\langle q\rangle'}{\partial t} = \frac{1}{\overline{\tau_c}}\left\{-u\frac{\partial q'}{\partial x} - v\frac{\partial q'}{\partial y} + C'\right\}; \tag{1a}$$

$$C' = -\langle\omega\frac{\partial q}{\partial p}\rangle' - P' + E', \tag{1b}$$

where q is specific humidity, and u, v, and ω are the zonal, meridional, and vertical pressure velocities, respectively. P and E are precipitation and evaporation, respectively. The angled brackets indicate a mass-weighted vertical integral from the surface to 100 hPa, and the prime symbol denotes intraseasonal (20–100 days) anomalies. C denotes the "column process" (Chikira, 2014), which includes vertical moisture advection, precipitation, and evaporation. C is obtained by taking the difference between total moisture tendency and the sum of the horizontal advection terms. $\overline{\tau c}$ is obtained using the following equation:

$$\overline{\tau c} = \frac{\overline{q_s}}{a\overline{P}}, \tag{2}$$

where $\overline{q_s}$ is column-integrated saturation specific humidity. Overbars in Equation 2 indicate 100-day low-pass filtered variables. The sensitivity parameter a is obtained from the nonlinear fit between column relative humidity and precipitation using data from each ensemble member, then averaged across all members (=7.8). To examine the relative roles of the mean state and MJO circulation anomalies, the meridional moisture advection term in Equation 1a is decomposed as:

$$-v\frac{\partial q}{\partial y} \cong -\overline{v}\frac{\partial\overline{q}}{\partial y} - \overline{v}\frac{\partial q'}{\partial y} - \overline{v}\frac{\partial q''}{\partial y} - v'\frac{\partial\overline{q}}{\partial y} - v'\frac{\partial q'}{\partial y} - v'\frac{\partial q''}{\partial y} - v''\frac{\partial\overline{q}}{\partial y} - v''\frac{\partial q'}{\partial y} - v''\frac{\partial q''}{\partial y}, \tag{3}$$

where the overbar and double prime denote the 100-day low-pass and 20-day high-pass filtered anomalies, respectively. The centered differencing scheme is used to represent the horizontal gradient and the budget results are not sensitive to the finite differencing scheme used (not shown).

For statistical significance testing for gridded data, we adopt the method proposed by Wilks (2016), which provides a strict p-value by employing the false discovery rate (FDR, Benjamini & Hochberg, 1995).

4. Results

Figure 1 presents the characteristics of MJO propagation in observations and the CESM2 ensemble simulations. The observed MJO precipitation anomalies move eastward from the IO to the western Pacific across the MC (Figure 1a). In CESM2, MC propagation metric values are obtained from one hundred and

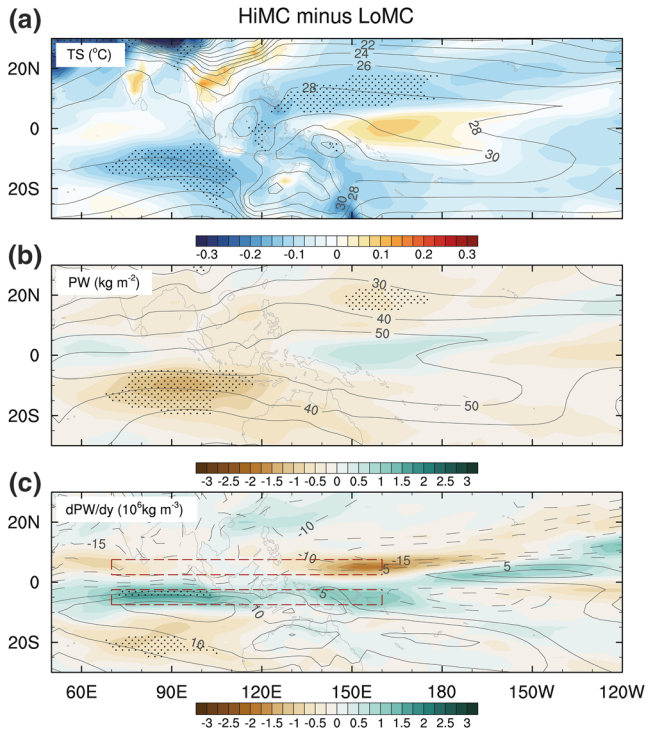

Figure 2. Climatology during boreal winter for 1850–2014 in the CESM2 ensemble mean (contour) and the difference between the composites of HiMC and LoMC (shaded). Each panel shows (a) surface temperature (°C), (b) precipitable water (kg m^{-2}), and (c) meridional gradient of precipitable water (10^6 kg m^{-3}). The linear trend of ensemble mean was removed before the composite. The red boxes indicate domains used for the MMG index. Areas with black dots indicate that that a statistically significant difference between HiMC and LoMC (p values = (a) 0.01, (b) 0.007, and (c) 0.004) using the two-sided Student's t-test adjusted by the FDR (α_{FDR} = 0.1).

forty-five 20-year moving windows for each ensemble member (see Figure S1 for the MC propagation metric of individual members). The results show a substantial low-frequency variability in the MC propagation metric ranging from 0.65 to 1.41 around the ensemble-mean, time-mean value of about 1 (Figure S1). The ensemble mean of the MC propagation metric does not show either a linear trend or noticeable low-frequency fluctuations during the historical periods, suggesting that their variability in individual ensemble members are predominantly due to the internal variability. In the following, we will examine the extent to which the internal variability in MJO characteristics in the CESM2 simulations is due to the differences in the mean state.

Motivated by the large internal variability, fifteen 20-year windows with the highest and lowest MC propagation metric values (HiMC and LoMC hereafter) are selected without allowing overlap between them. The selected thirty 20-year windows account for 36% (600/1,850 years) of the total years in the 10-member historical simulation. By design, the HiMC exhibits much stronger eastward propagation of the MJO convection (Figure 1f), in which the averaged MC propagation metric value is 81% greater than that for LoMC (Figure 1b).

The lag-longitude diagrams in Figure 1 also show anomalous moisture recharging (solid contours) before the peak of positive precipitation anomalies across the Indo-Pacific warm pool in both observations (Figure 1a) and the simulations (Figures 1d and 1e), indicating that the eastward propagation of MJO precipitation is coupled with that of moisture anomalies. Furthermore, Figure 1f shows that the greater MJO MC precipitation anomalies in HiMC can be traced to the greater moisture recharging locally, with about 10 days of lead time. It seems from Figure 1f that understanding the difference in moisture tendency at lag days −5 to 5 is the key to understand the abnormally strong MJO signature in the MC in HiMC.

Figure 2 shows boreal winter climatology in the ensemble mean (contours) and difference between HiMC and LoMC (shaded) for surface temperature, and precipitable water (PW) and its meridional gradient. In the climatology, the mean PW is meridionally confined near the equator to the west of the dateline (contours in Figure 2b), which corresponds to the positive (negative) meridional moisture gradient (MMG) to the south (north) of the equator (Figure 2c).

The mean surface temperature difference between HiMC and LoMC shows a significant cooling in the southeast IO and the northwest Pacific Ocean (Figure 2a). The pattern of the mean PW difference (Figure 2b) resembles that of surface temperature, showing slight wetter conditions to the east and west of the MC near the equator, and drier conditions at the off-equatorial MC regions especially in the Southern Hemisphere. As a result, the background MMG becomes steeper across the MC within the equatorial latitude band (10°S-10°N), where the difference in MJO propagation appears (Figure 1f). Note that the difference in the background moisture field shown in Figure 2 remains unchanged when calculated without strong MJO days presenting the MJO indices higher than 1.5 (Figure S2), and therefore is likely not due to the difference in MJO activity.

If the mean state difference in MMG in the MC can cause the difference in the rate of moistening before the onset of precipitation anomalies there, it would strongly support the notion that the difference between HiMC and LoMC in their MJO characteristics is due to the difference in the mean state MMG. To test this hypothesis, we define an MMG index using MMG values from regions where the notable MMG difference between HiMC and LoMC appears (red boxes in Figure 2c). We first calculate the averaged MMG over two zonally elongated areas in the warm pool slightly to the north (70°E-160°E, 2.5°N-7.5°N) and south

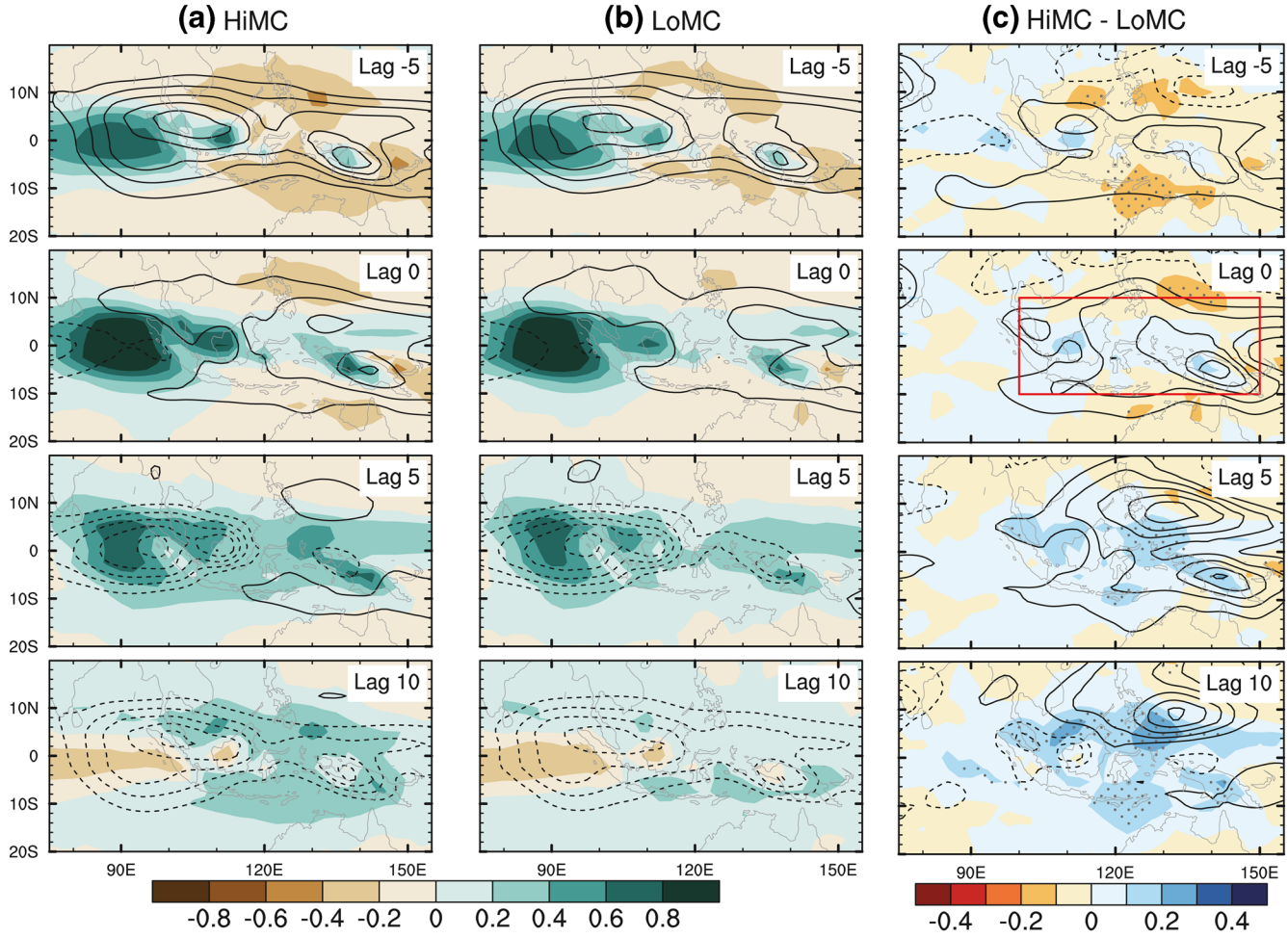

Figure 3. Lagged regression of 20–100 day band pass-filtered precipitation (shaded; mm day^{-1}) and column-integrated moisture tendency (contour; mm day^{-1}) regressed onto the precipitation averaged in the IO base point (85°E-95°E, 5°S-5°N). Each panel refers the composites of (a) HiMC, (b) LoMC, and (c) the difference between HiMC and LoMC. The contour intervals are 0.02 in (a) and (b), and 0.005 in (c). The red box on lag day 0 in Figure 3c indicates the MC domain used in Figure 4. Areas with black dots indicate that that a statistically significant difference between HiMC and LoMC (p-value = 0.008) using the two-sided Student's t-test adjusted by the FDR ($\alpha_{FDR} = 0.1$).

(70°E-160°E, 2.5°S-7.5°S) of the equator. Then the MMG index is obtained by subtracting the value for the northern box from that for the southern box. Since the MMG shows positive (negative) values in the southern (northern) box, a higher MMG index indicates a steeper meridional gradient in these regions. Figure 1c shows the MC propagation metric values of all individual 20-year windows binned by the MMG index. Overall, a steeper MMG tends to be associated with stronger MJO propagation across the MC. Also, consistent with Figure 2c, the background MMG in the HiMC windows are larger than that in the LoMC windows, although two LoMC windows show the background MMG greater than 1.8×10^7 kg m^{-3}. These results suggest that a steeper background MMG may be a necessary, but not a sufficient condition for stronger MJO propagation across the MC. In the next, we will examine how the steeper MMG in HiMC affects MJO convection over the MC region.

Figure 3 compares the horizontal patterns of precipitation (shaded) and moisture tendency (contours) anomalies at different lag days. On lag day −5, in both HiMC and LoMC, the MJO precipitation anomalies are centered around the eastern equatorial IO. As in observations, the 'vanguard' precipitation anomalies (Peatman et al., 2014) develop in Borneo and New Guinea islands during this time, which is slightly stronger in HiMC than in LoMC. As the MJO convection approaches the MC islands, HiMC shows stronger precipitation anomalies near the MC islands than those in LoMC (lag day 5). On lag day 10, the difference in precipitation anomalies are more pronounced over the MC region, particularly in the oceanic grid points

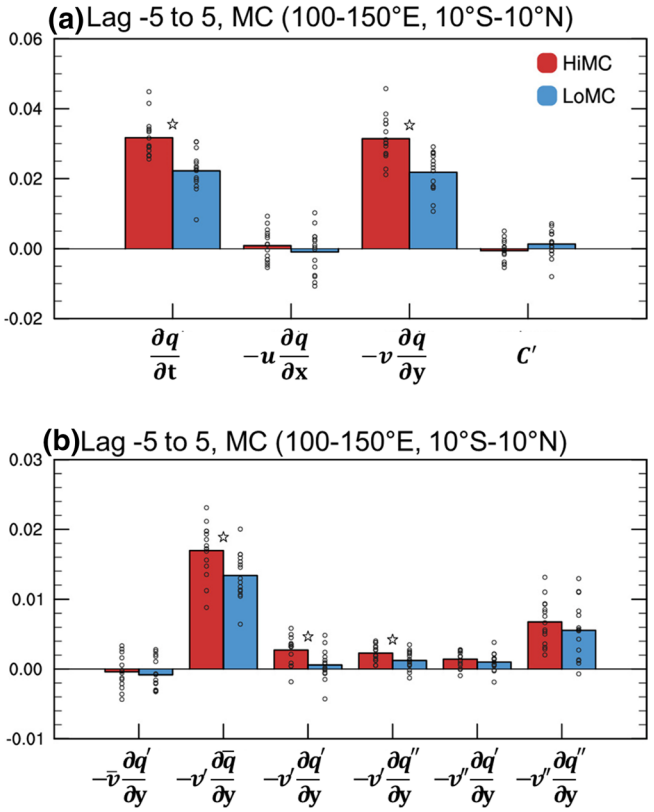

Figure 4. (a) Moisture budget terms averaged in the MC region (100°E-150°E, 10°S-10°N; the red box on lag day 0 in Figure 3c) on lag days from −5 to 5, regressed onto intraseasonal precipitation in the IO base point. (b) The meridional advection term decomposed into different time scale components of wind and moisture gradient. The decomposed terms of very small values are not shown. All terms shown in the bar graphs are column-integrated, 20–100 day band pass-filtered, and spatially weighted by the convective moisture adjustment frequency. The unit of the budget terms is converted to mm day^{-1} thereby the regression coefficient is unitless. The stars above the bars indicate statistically significant difference between HiMC and LoMC using the two-sided Student's *t*-test (*p*-value = 0.05).

surrounding the islands. The difference in precipitation anomalies is proceeded by the difference in moisture tendency, as in Figure 1f. In the MC region (100°E-150°E, 10°S-10°N; red box in Figure 3c), enhanced moistening around lag day 0 leads to the stronger precipitation anomalies on lag day 10.

To further examine moisture recharging processes over the MC region, in Figure 4 we compare the moisture budget terms. The higher total moisture tendency over the MC on lag days between −5 and 5 in HiMC can primarily be attributed to the meridional advection term (Figure 4a). The zonal advection and the column process terms are almost identical between HiMC and LoMC. Figure 4b shows the meridional advection term decomposed using different time scale components of horizontal wind and moisture gradient (Equation 3). The advection of the mean moisture by intraseasonal wind anomalies dominates the difference between HiMC and LoMC (second term in Figure 4b), indicating that the moisture recharging in the MC region is enhanced with a steeper background MMG. Many previous observational and modeling studies also emphasized the role of the mean state moisture gradient in that region (Ahn, Kim, Ham, & Park, 2020; DeMott et al., 2018, 2019; Jiang, 2017; Kim et al., 2014). The meridional advection of the intraseasonal moisture by intraseasonal wind anomalies also contributes to the difference in total meridional advection between HiMC and LoMC (third term in Figure 4b. The difference is likely due to the faster moistening near the equator associated with the stronger vanguard precipitation anomalies that provides a steeper anomalous intraseasonal moisture gradient in HiMC, which seems to be a consequence of the MJO-associated anomalies in HiMC being stronger there than those in LoMC. The high-frequency eddy term, which represents the effects of mixing between relatively moist near-equator and relatively dry subtropical air masses by synoptic-scale eddies (Andersen & Kuang, 2012; Maloney, 2009), also makes a small contribution to the total meridional advection, although the difference is not statistically significant (sixth term in Figure 4d).

5. Summary and Conclusion

Motivated by the recent studies highlighting the role of mean state moisture in the simulation of the MJO, we have examined the basic state and MJO propagation in a 10-member ensemble simulation made with a single model, the CESM2. Unlike the previous analysis of the multi-model ensembles (Ahn, Kim, Kang, et al., 2020; Gonzalez & Jiang, 2017; Jiang, 2017), in which the separation of the role of the mean state from that of the model physics is difficult, our assessment is unaffected by the differences in the parameterization schemes.

We found that the long-term simulations made with CESM2 showed a marked low-frequency variability in MJO propagation over the MC. The periods with stronger MJO propagation (HiMC) were distinguished from the periods of weaker MJO propagation (LoMC) by dry mean state anomalies in the off-equatorial MC corresponding to a steeper background MMG in the MC region. Examinations of the column water vapor anomalies associated with the MJO revealed that moisture recharging before the onset of MJO convection over the MC is much greater in HiMC than in LoMC, which is responsible for the stronger MJO propagation across the MC. The column-integrated moisture budget analysis further indicated that the anomalous moisture recharging over the MC region in HiMC is primarily associated with the meridional advection of mean moisture by MJO-perturbed wind.

Our results strongly support the notion that the background moisture gradient in the vicinity of MC plays an important role in the MJO (Gonzalez & Jiang, 2017; Jiang, 2017). Specifically, the steeper MMG in the

MC region is responsible for the larger moisture recharging ahead of MJO convection, resulting in the stronger propagation of the MJO (Ahn, Kim, Kang, et al., 2020; DeMott et al., 2019). Our results also demonstrated that changes in the mean state moisture gradient *alone* could lead to substantial changes to MJO propagation characteristics. Ahn, Kim, Ham, and Park (2020) perturbed a parameter in the cumulus convection scheme only over MC landmasses and examined the associated changes in the mean state and the MJO. They found changes in the mean state and MJO propagation over the oceanic area in the MC where the cumulus convection scheme is not altered, which cannot be attributed to the changes in the interaction between convection and its environment.

The considerable multi-decadal internal variability of the background MMG have implications for low-frequency variability of the MJO activity. Interannual to interdecadal variability of the MJO has been reported both in simulations (Schubert et al., 2013) and in observations (Gonzalez & Jiang, 2019; Pohl & Matthews, 2007; Slingo et al., 1999), at least part of which can be explained by the influence of mean state moisture on MJO propagation. Additionally, the assessment of MJO fidelity in the multimodel intercomparison studies might be partly interfered by the internally varying basic state because most studies use a single ensemble member and a period of equal or less than 20 years (Ahn et al., 2017 Ahn, Kim, Kang, et al., 2020; Gonzalez & Jiang, 2017; Hung et al., 2013; Jiang, 2017; Kim et al., 2009; Ling et al., 2017, 2019). Our results demonstrate the potential added value of evaluating multiple realizations of the same model when available (e.g., as in PCMDI metrics package (Gleckler et al., 2016); https://pcmdi.llnl.gov/research/metrics/mjo). Future studies of how the mean moisture field is modulated by low-frequency climate variability are warranted for further understanding of the interaction between the basic state and the MJO.

There have been attempts to isolate the effects of parameterization changes from that of changes in the mean state (Kelly et al., 2017; Peatman et al., 2018). Using a primitive equation model with no representation of surface turbulent and radiative fluxes, Kelly et al. (2017) constrained the mean state with time-independent forcing and linearized convective heating and moistening processes using the linear response function of Kuang (2010). That way, they could make changes in the convective processes with minimal impacts on the mean state. In a series of aquaplanet simulations, Peatman et al. (2018) examined the effects of moisture entrainment on convectively coupled equatorial waves with the basic state humidity being constrained. The modeling framework proposed in these studies can potentially be used to study the role of the mean state independent of the effect of parameterization changes, although in both studies constraining the mean state was found to be difficult. Further work is needed to improve the modeling framework that is suitable to study the role of the mean state on tropical waves.

Acknowledgments
We thank the anonymous reviewers for their constructive comments, which greatly helped improve earlier versions of the paper. This work was funded by the NOAA CVP program (NA18OAR4310300), the DOE RGMA program (DE-SC0016223), the NASA MAP program (80NSSC17K0227), and the KMA R&D program (KMI2018-03110). Work of LLNL-affiliated authors was performed under the auspices of the U.S. Department of Energy by Lawrence Livermore National Laboratory under Contract DE-AC52-07NA27344 and their efforts were supported by the Regional and Global Climate Modeling Program of the United States Department of Energy's Office of Science. We acknowledge the World Climate Research Programme, which, through its Working Group on Coupled Modelling, coordinated and promoted CMIP6. We thank the climate modeling groups for producing and making available their model output, the Earth System Grid Federation (ESGF) for archiving the data and providing access, and the multiple funding agencies who support CMIP6 and ESGF. We thank DOE's RGMA program area, the Data Management program, and NERSC for making this coordinated CMIP6 analysis activity possible.

Data Availability Statement

The CESM2 historical simulation data was obtained from the CMIP6 archive (https://esgf-node.llnl.gov/search/cmip6/). The TRMM provided the precipitation data (https://gpm.nasa.gov/data/directory). The ECMWF provided the fifth generation of ECMWF reanalysis (ERA5, https://www.ecmwf.int/en/forecasts/datasets/reanalysis-datasets/era5).

References

Adames, Á. F. (2017). Precipitation budget of the Madden–Julian oscillation. *Journal of the Atmospheric Sciences*, *74*(6), 1799–1817.

Adames, Á. F., & Kim, D. (2016). The MJO as a dispersive, convectively coupled moisture wave: Theory and observations. *Journal of the Atmospheric Sciences*, *73*(3), 913–941.

Ahn, M. S., Kim, D., Ham, Y. G., & Park, S. (2020). Role of Maritime Continent land convection on the mean state and MJO propagation. *Journal of Climate*, *33*(5), 1659–1675.

Ahn, M. -S., Kim, D., Kang, D., Lee, J., Sperber, K. R., Gleckler, P. J. (2020). MJO propagation across the Maritime Continent: Are CMIP6 models better than CMIP5 models? *Geophysical Research Letters*, *47*, e2020GL087250. https://doi.org/10.1029/2020GL087250

Ahn, M. S., Kim, D., Park, S., & Ham, Y. G. (2019). Do we need to parameterize mesoscale convective organization to mitigate the MJO-mean state trade-off? *Geophysical Research Letters*, *46*(4), 2293–2301. https://doi.org/10.1029/2018GL080314

Ahn, M.-S., Kim, D., Sperber, K. R., Kang, I.-S., Maloney, E., Waliser, D., & Hendon, H. (2017). MJO simulation in CMIP5 climate models: MJO skill metrics and process-oriented diagnosis. *Climate Dynamics*, *49*(11–12), 4023–4045. https://doi.org/10.1007/s00382-017-3558-4

Andersen, J. A., & Kuang, Z. (2012). Moist static energy budget of MJO-like disturbances in the atmosphere of a zonally symmetric aquaplanet. *Journal of Climate*, *25*(8), 2782–2804. https://doi.org/10.1175/JCLI-D-11-00168.1

Benjamini, Y., & Hochberg, Y. (1995). Controlling the false discovery rate: A practical and powerful approach to multiple testing. *Journal of the Royal Statistical Society: Series B (Methodological)*, *57*(1), 289–300.

Chikira, M. (2014). Eastward-propagating intraseasonal oscillation represented by Chikira–Sugiyama cumulus parameterization. Part II: Understanding moisture variation under weak temperature gradient balance. *Journal of the Atmospheric Sciences*, *71*(2), 615–639.

Danabasoglu, G., Lamarque, J. -F., Bacmeister, J., Bailey, D. A., DuVivier, A. K., Edwards, J. (2020). The Community Earth System Model Version 2 (CESM2). *Journal of Advances in Modeling Earth Systems*, *12*(2), 1–35. https://doi.org/10.1029/2019MS001916

DeMott, C. A., Klingaman, N. P., Tseng, W. L., Burt, M. A., Gao, Y., & Randall, D. A. (2019). The convection connection: How ocean feedbacks affect tropical mean moisture and MJO propagation. *Journal of Geophysical Research: Atmospheres*, *124*(22), 11910–11931. https://doi.org/10.1029/2019JD031015

DeMott, C. A., Wolding, B. O., Maloney, E. D., & Randall, D. A. (2018). Atmospheric mechanisms for MJO decay over the Maritime Continent. *Journal of Geophysical Research: Atmospheres*, *123*(10), 5188–5204. https://doi.org/10.1029/2017JD026979

Eyring, V., Bony, S., Meehl, G. A., Senior, C. A., Stevens, B., Stouffer, R. J., & Taylor, K. E. (2016). Overview of the Coupled Model Intercomparison Project Phase 6 (CMIP6) experimental design and organization. *Geoscientific Model Development*, *9*(5), 1937–1958.

Gleckler, P., Doutriaux, C., Durack, P. J., Taylor, K. E., Zhang, Y., Williams, D. N. (2016). A more powerful reality test for climate models. *Eos*, *97*. https://doi.org/10.1029/2016EO051663

Gonzalez, A. O., & Jiang, X. (2017). Winter mean lower tropospheric moisture over the Maritime Continent as a climate model diagnostic metric for the propagation of the Madden-Julian oscillation. *Geophysical Research Letters*, *44*(5), 2588–2596. https://doi.org/10.1002/2016GL072430

Gonzalez, A. O., & Jiang, X. (2019). Distinct propagation characteristics of intraseasonal variability over the tropical west Pacific. *Journal of Geophysical Research: Atmospheres*, *124*(10), 5332–5351. https://doi.org/10.1029/2018JD029884

Hersbach, H., Bell, B., Berrisford, P., Horányi, A., Sabater, J. M., Nicolas, J. (2019). Global reanalysis: Goodbye ERA-Interim, hello ERA5. *ECMWF Newsletter*, *159*, 17–24. https://doi.org/10.21957/vf291hehd7

Holton, J. R., & Hakim, G. J. (2013). Chapter 5—Atmospheric oscillations: Linear perturbation theory. In J. R. Holton & G. J. Hakim (Eds.), *An introduction to dynamic meteorology* (5th ed., pp. 127–170). Boston, MA: Academic Press. https://doi.org/10.1016/B978-0-12-384866-6.00005-2

Huffman, G. J., Bolvin, D. T., Nelkin, E. J., Wolff, D. B., Adler, R. F., Gu, G. (2007). The TRMM Multisatellite Precipitation Analysis (TMPA): Quasi-global, multiyear, combined-sensor precipitation estimates at fine scales. *Journal of Hydrometeorology*, *8*(1), 38–55. https://doi.org/10.1175/JHM560.1

Hung, M.-P., Lin, J.-L., Wang, W., Kim, D., Shinoda, T., & Weaver, S. J. (2013). MJO and convectively coupled equatorial waves simulated by CMIP5 climate models. *Journal of Climate*, *26*(17), 6185–6214. https://doi.org/10.1175/JCLI-D-12-00541.1

Inness, P. M., Slingo, J. M., Woolnough, S. J., Neale, R. B., & Pope, V. D. (2001). Organization of tropical convection in a GCM with varying vertical resolution; implications for the simulation of the Madden-Julian oscillation. *Climate Dynamics*, *17*(10), 777–793.

Jiang, X. (2017). Key processes for the eastward propagation of the Madden-Julian oscillation based on multimodel simulations. *Journal of Geophysical Research: Atmospheres*, *122*(2), 755–770. https://doi.org/10.1002/2016JD025955

Jiang, X., Waliser, D. E., Xavier, P. K., Petch, J., Klingaman, N. P., Woolnough, S. J. (2015). Vertical structure and physical processes of the Madden-Julian oscillation: Exploring key model physics in climate simulations. *Journal of Geophysical Research: Atmospheres*, *120*(10), 4718–4748. https://doi.org/10.1002/2014JD022375

Jones, C., Waliser, D. E., Lau, K. M., & Stern, W. (2004). The Madden–Julian oscillation and its impact on Northern Hemisphere weather predictability. *Monthly Weather Review*, *132*(6), 1462–1471. https://doi.org/10.1175/1520-0493(2004)132<1462:TMOAII>2.0.CO;2

Kelly, P., Mapes, B., Hu, I., Song, S., & Kuang, Z. (2017). Tangent linear superparameterization of convection in a 10 layer global atmosphere with calibrated climatology. *Journal of Advances in Modeling Earth Systems*, *9*(2), 932–948. https://doi.org/10.1002/2016MS000871

Kim, D., Kug, J.-S., & Sobel, A. H. (2014). Propagating versus nonpropagating Madden–Julian oscillation events. *Journal of Climate*, *27*(1), 111–125. https://doi.org/10.1175/JCLI-D-13-00084.1

Kim, D., & Maloney, E. D. (2017). Review: Simulation of the Madden-Julian oscillation using general circulation models. In C.-P. Chang, H.-C. Kuo, N.-C. Lau, R. H. Johnson, B. Wang, & M. C. Wheeler (Eds.), *The global monsoon system* (3rd ed., pp. 119–131). Singapore: World Scientific. https://doi.org/10.1142/9789813200913_0009

Kim, D., Sobel, A. H., Maloney, E. D., Frierson, D. M., & Kang, I. S. (2011). A systematic relationship between intraseasonal variability and mean state bias in AGCM simulations. *Journal of Climate*, *24*(21), 5506–5520.

Kim, D., Sperber, K., Stern, W., Waliser, D., Kang, I.-S., Maloney, E. (2009). Application of MJO simulation diagnostics to climate models. *Journal of Climate*, *22*(23), 6413–6436. https://doi.org/10.1175/2009JCLI3063.1

Kiranmayi, L., & Maloney, E. D. (2011). Intraseasonal moist static energy budget in reanalysis data. *Journal of Geophysical Research: Atmospheres*, *116*(D21). https://doi.org/10.1029/2011jd016031

Kuang, Z. (2010). Linear response functions of a cumulus ensemble to temperature and moisture perturbations and implications for the dynamics of convectively coupled waves. *Journal of the Atmospheric Sciences*, *67*(4), 941–962.

Ling, J., Zhang, C., Wang, S., & Li, C. (2017). A new interpretation of the ability of global models to simulate the MJO. *Geophysical Research Letters*, *44*(11), 5798–5806. https://doi.org/10.1002/2017GL073891

Ling, J., Zhao, Y., & Chen, G. (2019). Barrier effect on MJO propagation by the Maritime Continent in the MJO task force/GEWEX atmospheric system study models. *Journal of Climate*, *32*(17), 5529–5547. https://doi.org/10.1175/jcli-d-18-0870.1

Madden, R. A., & Julian, P. R. (1971). Detection of a 40–50 day oscillation in the zonal wind in the tropical Pacific. *Journal of the Atmospheric Sciences*, *28*(5), 702–708. https://doi.org/10.1175/1520-0469(1971)028%3C0702:DOADOI%3E2.0.CO;2

Madden, R. A., & Julian, P. R. (1972). Description of global-scale circulation cells in the tropics with a 40–50 day period. *Journal of the Atmospheric Sciences*, *29*(6), 1109–1123. https://doi.org/10.1175/1520-0469(1972)029<1109:DOGSCC>2.0.CO;2

Maloney, E. D. (2009). The moist static energy budget of a composite tropical intraseasonal oscillation in a climate model. *Journal of Climate*, *22*(3), 711–729. https://doi.org/10.1175/2008JCLI2542.1

Mapes, B., & Neale, R. (2011). Parameterizing convective organization to escape the entrainment dilemma. *Journal of Advances in Modeling Earth Systems*, *3*(2), M06004. https://doi.org/10.1029/2011MS000042

Neena, J. M., Lee, J. Y., Waliser, D., Wang, B., & Jiang, X. (2014). Predictability of the Madden–Julian oscillation in the Intraseasonal Variability Hindcast Experiment (ISVHE). *Journal of Climate*, *27*(12), 4531–4543. https://doi.org/10.1175/JCLI-D-13-00624.1

Peatman, S. C., Matthews, A. J., & Stevens, D. P. (2014). Propagation of the Madden-Julian oscillation through the Maritime Continent and scale interaction with the diurnal cycle of precipitation. *Quarterly Journal of the Royal Meteorological Society*, *140*(680), 814–825. https://doi.org/10.1002/qj.2161

Peatman, S. C., Methven, J., & Woolnough, S. J. (2018). Isolating the effects of moisture entrainment on convectively coupled equatorial waves in an aquaplanet GCM. *Journal of the Atmospheric Sciences*, *75*(9), 3139–3157. https://doi.org/10.1175/JAS-D-18-0098.1

Pohl, B., & Matthews, A. J. (2007). Observed changes in the lifetime and amplitude of the Madden–Julian oscillation associated with interannual ENSO sea surface temperature anomalies. *Journal of Climate*, *20*(11), 2659–2674. https://doi.org/10.1175/JCLI4230.1

Raymond, D. J., & Fuchs, Ž. (2009). Moisture modes and the Madden–Julian oscillation. *Journal of Climate*, *22*(11), 3031–3046.

Schubert, J. J., Stevens, B., & Crueger, T. (2013). Madden-Julian oscillation as simulated by the MPI Earth system model: Over the last and into the next millennium. *Journal of Advances in Modeling Earth Systems*, *5*(1), 71–84. https://doi.org/10.1029/2012MS000180

Slingo, J. M., Rowell, D. P., Sperber, K., & Nortley, F. (1999). On the predictability of the interannual behaviour of the Madden-Julian oscillation and its relationship with El Niño. *Quarterly Journal of the Royal Meteorological Society*, *125*(554), 583–609. https://doi.org/10.1256/smsqj.55410

Slingo, J. M., Sperber, K. R., Boyle, J. S., Ceron, J. P., Dix, M., Dugas, B., (1996). Intraseasonal oscillations in 15 atmospheric general circulation models: Results from an AMIP diagnostic subproject. *Climate Dynamics*, *12*(5), 325–357.

Sobel, A., & Maloney, E. (2012). An idealized semi-empirical framework for modeling the Madden–Julian oscillation. *Journal of the Atmospheric Sciences*, *69*(5), 1691–1705.

Sobel, A., & Maloney, E. (2013). Moisture modes and the eastward propagation of the MJO. *Journal of the Atmospheric Sciences*, *70*(1), 187–192.

Sobel, A., Wang, S., & Kim D. (2014). Moist Static Energy Budget of the MJO during DYNAMO. *Journal of the Atmospheric Sciences*, *71*(11), 4276–4291. https://doi.org/10.1175/jas-d-14-0052.1

Wilks, D. (2016). "The stippling shows statistically significant grid points": How research results are routinely overstated and overinterpreted, and what to do about it. *Bulletin of the American Meteorological Society*, *97*(12), 2263–2273.

Zhang, C. (2013). Madden-Julian oscillation: Bridging weather and climate. *Bulletin of the American Meteorological Society*, *94*(12), 1849–1870. https://doi.org/10.1175/BAMS-D-12-00026.1